Size-Selective Photoetching of Nanocrystalline Semiconductor Particles

A. van Dijken,* A. H. Janssen, M. H. P. Smitsmans, D. Vanmaekelbergh, and A. Meijerink

Debye Institute, Utrecht University, PO Box 80.000, 3508 TA Utrecht, The Netherlands

Received April 22, 1998. Revised Manuscript Received July 22, 1998

An overview is presented of size-selective photoetching experiments on nanocrystalline semiconductor particles. Four different compounds (CdS, ZnS, PbS, and ZnO) have been prepared by standard colloid−chemical synthetic methods. For CdS, the initial mean radius of 35 Å could be gradually decreased to 7.5 Å by size-selective photoetching. The adjustment of the particle size can be controlled to a high degree by varying the wavelength of the light that is used. It is also shown that the particle size distribution narrows during the photoetching process from about 40% to 10−15%. For ZnS and ZnO, only the feasibility of the technique could be demonstrated. This is due to the fact that these compounds have very large band gaps which limit the range for photoetching experiments. The initial radius of the ZnO particles was approximately 30−35 Å and could be decreased to about 15 Å, again accompanied by a narrowing of the particle size distribution. For PbS, no concrete evidence was obtained for the feasibility of size-selective photoetching.

I. Introduction

It is well-known that semiconductors exhibit quantum size effects when the size of the solid particle is smaller than the bulk exciton radius as a result of the spatial confinement of the charge carriers.[1−3] Two of these quantum size effects are the shift of the absorption onset to higher energies (often referred to as an increase of the band gap) and the transition from energy bands to discrete energy levels. These phenomena are mainly responsible for the increased interest in quantum-confined systems over the last couple of years.[2−7]

Several techniques that allow the preparation of semiconductor particles with nanometer sizes are based on sol−gel methods. They have been reported for the preparation of various semiconductor particles, such as CdS,[2,8] ZnS,[2,4] PbS,[2,11] ZnO,[2,12−15] and TiO_2.[12,16,17]

To study the size-dependent properties it is important to have monodisperse suspensions of different particle sizes. To achieve this one can basically use two different approaches. In the first of these, the preparation method itself determines the particle size and size distribution. These methods are based on preparation inside a limited space, such as a cavity in a zeolite[18−20] or an inverse micelle in solution.[21−23] The second approach starts with a sol−gel preparation, followed by treatments to separate different particle sizes from the initial size distribution. These treatments include exclusion chromatography,[24] gel electrophoresis,[25] and size-selective precipitation.[26−28] In general, preparation inside an inverse micelle yields a size distribution of about 10−25%,[22] while a preparation followed by size-selective precipitation gives a dispersity of 5−10%.[28,29]

(1) Brus, L. *J. Phys. Chem.* **1986**, *90*, 2555.
(2) Henglein, A. *Top. Curr. Chem.* **1988**, *143*, 113.
(3) Henglein, A. *Chem. Rev.* **1989**, *89*, 1861.
(4) Weller, H.; Koch, U.; Gutiérrez, M.; Henglein, A. *Ber. Bunsen-Ges. Phys. Chem.* **1984**, *88*, 649.
(5) Henglein, A. *Ber. Bunsen-Ges. Phys. Chem.* **1982**, *86*, 301.
(6) Wang, Y.; Herron, N. *J. Phys. Chem.* **1991**, *95*, 525.
(7) Weller, H. *Angew. Chem., Int. Ed. Engl.* **1993**, *32*, 41.
(8) Henglein, A.; Fojtik, A.; Weller, H. *Ber. Bunsen-Ges. Phys. Chem.* **1987**, *91*, 441.
(9) Meissner, D.; Memming, R.; Shuben, L.; Yesodharan, S.; Grätzel, M. *Ber. Bunsen-Ges. Phys. Chem.* **1985**, *89*, 121.
(10) Vossmeyer, T.; Katsikas, L.; Giersig, M.; Popovic, I. G.; Diesner, K.; Chemseddine, A.; Eychmüller, A.; Weller, H. *J. Phys. Chem.* **1994**, *98*, 7665.
(11) Gallardo, S.; Gutiérrez, M.; Henglein, A.; Janata, E. *Ber. Bunsen-Ges. Phys. Chem.* **1989**, *93*, 1080.
(12) Bahnemann, D. W. *Israel J. Chem.* **1993**, *33*, 115.
(13) Bahnemann, D. W.; Kormann, C.; Hoffmann, M. R. *J. Phys. Chem.* **1987**, *91*, 3789.
(14) Haase, M.; Weller, H.; Henglein, A. *J. Phys. Chem.* **1988**, *92*, 482.
(15) Spanhel, L.; Anderson, M. A. *J. Am. Chem. Soc.* **1991**, *113*, 2826.
(16) Bahnemann, D. W.; Henglein, A.; Lilie, J.; Spanhel, L. *J. Phys. Chem.* **1984**, *88*, 709.
(17) Kormann, C.; Bahnemann, D. W.; Hoffmann, M. R. *J. Phys. Chem.* **1988**, *92*, 5196.
(18) Chen, W.; Wang, Z. G.; Lin, Z. J.; Qian, J. J.; Lin, L. Y. *Solid State Commun.* **1996**, *100*, 101.
(19) Chen, W.; Wang, Z. G.; Lin, Z. J.; Qian, J. J.; Lin, L. Y. *Appl. Phys. Lett.* **1996**, *68(14)*, 1990.
(20) Wang, Y.; Herron, N. *J. Phys. Chem.* **1987**, *91*, 257.
(21) Counio, G.; Esnouf, S.; Gacoin, T.; Boilot, J.-P. *J. Phys. Chem.* **1996**, *100*, 20021.
(22) Steigerwald, M. L.; Alivisatos, A. P.; Gibson, J. M.; Harris, T. D.; Kortan, R.; Muller, A. J.; Thayer, A. M.; Duncan, T. M.; Douglas, D. C.; Brus, L. E. *J. Am. Chem. Soc.* **1988**, *110*, 3046.
(23) Kortan, A. R.; Hull, R.; Opila, R. L.; Bawendi, M. G.; Steigerwald, M. L.; Carroll, P. J.; Brus, L. E. *J. Am. Chem. Soc.* **1990**, *112*, 1327.
(24) Fischer, C. H.; Weller, H.; Katsikas, L.; Henglein, A. *Langmuir* **1989**, *5*, 429.
(25) Eychmüller, A.; Katsikas, L.; Weller, H. *Langmuir* **1990**, *6*, 1605.
(26) Murray, C. B.; Norris, D. J.; Bawendi, M. G. *J. Am. Chem. Soc.* **1993**, *115*, 8706.
(27) Bawendi, M. G.; Carroll, P. J.; Wilson, W. L.; Brus, L. E. *J. Chem. Phys.* **1992**, *96(2)*, 946.
(28) Norris, D. J.; Bawendi, M. G. *Phys. Rev. B* **1996**, *53* (24), 16338.

10.1021/cm980715p CCC: $15.00
Published on Web 09/10/1998

Recently a novel technique has been described that allows the particle size to be adjusted after preparation by photoetching the semiconductor particles to a size which is determined by the wavelength of the light. The first observations in this direction were made by Henglein et al., who showed that semiconductor particles can be photoetched via an electroless mechanism.[5] The size-selectivity of the technique was first demonstrated for nanocrystalline CdS particles by Matsumoto et al.[30,31] We have shown that these results can be extended toward much smaller particle size.[32] With respect to other sulfides such as ZnS and PbS, no size-selective-photoetching experiments have been described before. In this paper we give an overview of the results that we have obtained with size-selective photoetching of nanocrystalline semiconductor particles. It is shown that for CdS the particle radius can be gradually decreased to 7.5 Å. Information about the particle size is obtained by performing TEM and XRD measurements and by analyzing the absorption spectra. From this analysis it is also possible to give an estimation of the particle size distribution. We have also applied the technique of size-selective photoetching to ZnS, PbS, and ZnO.

II. Theory of Size-Selective Photoetching

When a semiconductor is illuminated with light that has an energy which exceeds that of the band gap, absorption can take place, and electron−hole pairs are created. The electron can subsequently recombine with the hole, either radiatively or nonradiatively. Radiative recombination can give rise to a relatively sharp emission band centered at approximately the band gap energy (exciton recombination band) and/or a relatively broad emission band centered at lower energies when (deep) traps are involved in the recombination process. In the case of nanocrystalline particles of CdS and ZnO, both these emission bands can be observed at room temperature. Due to a large surface-to-volume ratio, nonradiative recombination via surface traps is the predominant route.

When the recombination of electron−hole pairs can be prohibited by removing the electron (by an interfacial process), the hole can be used to dissolve the semiconductor. This well-known process of electroless photoetching,[33−35] in combination with the shift of the absorption onset to higher energies upon a decrease of the particle size, provides the basis for the technique of size-selective photoetching.

Removal of the electron from a semiconductor particle can be achieved by using electron scavengers such as oxygen molecules or methylviologen ions (MV^{2+}) that are adsorbed on the surface of the particle. Methylviologen shuttles the photogenerated electrons from the semiconductor particle to the adsorbed oxygen molecules. First, the electrons are efficiently scavenged from the conduction band, resulting in the formation of $MV^{+\bullet}$ radicals, followed by the reduction of oxygen and regeneration of MV^{2+}. As a result, the use of methylviologen can increase the rate of the photoetching process.[31,32]

One can take as a threshold for the occurrence of quantum size effects the value for the Bohr radius of the exciton in the bulk material (a_B^{exc}, in Å):

$$a_B^{exc} = 0.529\epsilon_\infty\left(\frac{1}{m_e^*}\frac{1}{m_h^*}\right) \quad (1)$$

In eq 1, ϵ_∞ is the high-frequency relative dielectric constant while m_e* and m_h* are the effective masses of the electron and hole, respectively (both in units m_e).

When the radius of a semiconductor particle has decreased below a_B^{exc}, the energy for the lowest electronic transition can be calculated using the following equation, based on the quantum mechanical model of a particle in a spherical box with infinite potential energy barriers:[1]

$$E = E_g + \frac{h^2}{8m_eR^2}\left(\frac{1}{m_e^*} + \frac{1}{m_h^*}\right) - \frac{1.8e^2}{4\pi\epsilon_\infty\epsilon_0} \quad (2)$$

In eq 2 E_g represents the band gap energy for the bulk semiconductor, m_e* and m_h* are the effective masses of the electron and hole, respectively (both in units m_e), R is the radius of the semiconductor particle, and ϵ_∞ is the high-frequency relative dielectric constant of the material. The R^{-2}-term is a confinement energy term, while the R^{-1}-term reflects the Coulomb interaction between electrons and holes. In Figure 1a, the dependence of E on the particle size as given by eq 2 is shown schematically. When semiconductor particles from a distribution as shown in Figure 1b are illuminated with light of energy $h\nu_1$, only the particles that are 50 Å or bigger will be able to absorb the light. These particles can be photoetched, which will result in an increase of their band gap energy. Gradually the size of these particles will be such that the band gap energy is larger than the photon energy. At this particle size, determined by the wavelength of the light, the photoetching will stop. The initial size distribution should now have changed to that shown in Figure 1c. In the same way one can further decrease the particle size by using light of a higher energy (e.g. $h\nu_2$; see Figure 1d).

To demonstrate the technique of size-selective photoetching as shown in Figure 1, nanocrystalline CdS particles can be used as a model system. This system has been studied very extensively in the literature.[2,10,36−38] The overall photodissolution reaction is very well-known:[9]

(29) Chemseddine, A.; Weller, H. *Ber. Bunsen-Ges. Phys. Chem.* **1993**, *97*, 636.
(30) Matsumoto, H.; Sakata, T.; Mori, H.; Yoneyama, H. *Chem. Lett.* **1995**, 595.
(31) Matsumoto, H.; Sakata, T.; Mori, H.; Yoneyama, H. *J. Phys. Chem.* **1996**, *100*, 13781.
(32) Van Dijken, A.; Vanmaekelbergh, D.; Meijerink, A. *Chem. Phys. Lett.* **1997**, *269*, 494.
(33) Meissner, D.; Benndorf, C.; Memming, R. *Appl. Surf. Sci.* **1987**, *27*, 423.
(34) Meissner, D.; Memming, R.; Kastening, B. *J. Phys. Chem.* **1988**, *92*, 3476.
(35) Notten, P. H. L.; Van den Meerakker, J. E. A. M.; Kelly, J. J. *Etching of III−V Semiconductors. An Electrochemical Approach*; Elsevier Advanced Technology: Oxford, 1991.
(36) Fojtik, A.; Weller, H.; Koch, U.; Henglein, A. *Ber. Bunsen-Ges. Phys. Chem.* **1984**, *88*, 969.
(37) Eychmüller, A.; Hässelbarth, A.; Katsikas, L.; Weller, H. *J. Lumin.* **1991**, *48&49*, 745.
(38) Tittel, J.; Göhde, W.; Koberling, F.; Basché, Th.; Kornowski, A.; Weller, H.; Eychmüller, A. *J. Phys. Chem. B* **1997**, *101*, 3013.

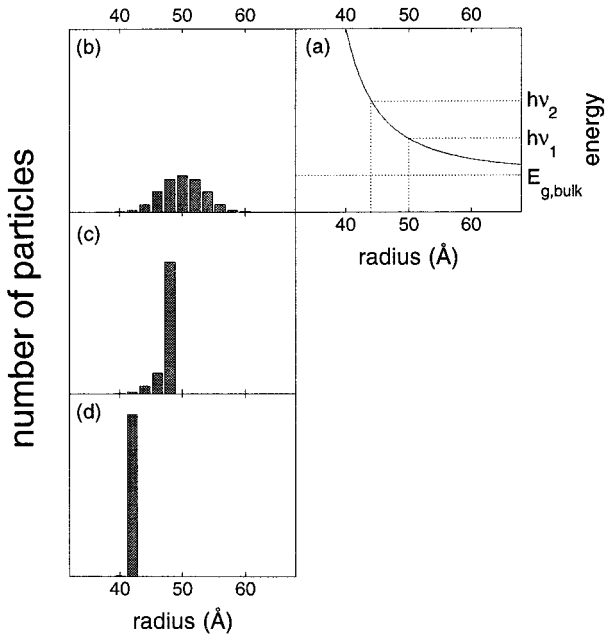

Figure 1. Schematic picture of the concept of size-selective photoetching: (a) band gap energy as a function of particle radius for an arbitrary semiconductor, (b) initial size distribution, (c) size distribution after photoetching with light of energy $h\nu_1$, (d) size distribution after photoetching with light of energy $h\nu_2$.

$$CdS + 2O_2 \xrightarrow{nh\nu} Cd^{2+} + SO_4^{2-}$$

Illumination of CdS particles with photons whose energy exceeds that of the band gap leads to the formation of electron−hole pairs. Adsorbed oxygen can be reduced by electrons from the conduction band while the holes in the valence band lead to a dissolution of CdS. The efficiency of this process is low since the majority of the electron−hole pairs will recombine, either radiatively or nonradiatively.

To determine the particle size after size-selective photoetching, techniques such as transmission electron microscopy (TEM) and X-ray diffraction (XRD) can be used. The width of a diffraction peak increases as the size of the crystallites decreases. The Scherrer formula can be used to determine the size (*s*) of the crystallite, which is equal to the diameter of the semiconductor particle:

$$s = \frac{0.9\lambda}{B \cos \theta_B} \qquad (3)$$

In eq 3, λ is the wavelength of the X-rays (for Cu Kα_1 this is 1.541 Å), B is the fwhm of the diffraction peak (in radians), and θ_B is the maximum of the diffraction peak (in radians). Apart from these experimental techniques, empirical relationships between the mean particle radius and the position of the first absorption maximum can also be used. Such relationships have been established in the literature for CdS[10] and ZnO,[14] and they will be used here instead of eq 2, although there is a reasonable agreement between the values obtained by both methods.

Finally, to measure the narrowing of the particle size distribution after size-selective photoetching, the width of the inhomogeneously broadened bands in the absorption and emission spectra can be analyzed.

III. Experimental Section

CdS.[36,37] To obtain a colloidal suspension of nanocrystalline CdS particles, 20 mL of an aqueous solution of 0.05 M sodium polyphosphate was added to 40 mL of an aqueous solution of 0.01 M $Cd(ClO_4)_2 \cdot 6H_2O$. After diluting this solution to 100 mL, 7.2 mL of H_2S (Aldrich lecture bottle, 99.5+%) was injected using an airtight syringe. Vigorously shaking the sample for several minutes at room temperature resulted in a transparent yellow suspension. According to the literature, this preparation of an aqueous CdS suspension should yield particles with a mean radius of about 35 Å.[37]

ZnS.[4] A colloidal suspension of nanocrystalline ZnS particles was obtained by diluting 5 mL of an aqueous solution of 0.01 M $Zn(ClO_4)_2 \cdot 6H_2O$ to 100 mL before adding 10 mL of an aqueous solution of 0.05 M sodium polyphosphate. After injection of 1 mL of H_2S, the sample was vigorously shaken for several minutes at room temperature and allowed to age for 1 day. The resulting colloidal suspension was transparent and colorless.

PbS.[11] For this suspension a mixture of 2 mL of an aqueous solution of 0.005 M $Pb(ClO_4)_2 \cdot 3H_2O$ and 2 mL of an aqueous solution of 0.5 M poly(vinyl alcohol) was diluted to 100 mL before injecting 215 μL of H_2S. This resulted in a transparent, dark red colloidal suspension. According to the literature,[11] the PbS particles have a rodlike shape with a length of 180 Å and a diameter of 15−25 Å.

ZnO.[13] A solution of 0.06 g ($2.7 \cdot 10^{-4}$ mol) of $Zn(OAc)_2 \cdot 2H_2O$ in 80 mL of 2-propanol was made at 50 °C. After dilution of the solution to 230 mL with 2-propanol, it was cooled to 0 °C. At this temperature, 20 mL of a solution of 0.082 g ($2.0 \cdot 10^{-3}$ mol) of NaOH in 100 mL of 2-propanol was added within 1 min while the mixture was stirred. After aging in a water bath at 65 °C for 2 h a transparent, colorless suspension of ZnO particles was obtained. According to the literature,[13] the ZnO particles are almost spherical and have a mean radius of 25 Å and a relatively narrow particle size distribution (ΔR = 5 Å).

Since alcohols can act as hole scavengers, photoetching of ZnO could not be performed in the solvent in which ZnO was prepared. Therefore, the ZnO particles were transferred to water before photoetching. This was done by first adsorbing the ZnO particles on a silica powder (Aerosil Ox50 Degussa). After centrifuging of the suspension and washing of the precipitate, the ZnO particles—still adsorbed on silica—were redispersed in water.

Photoetching. The size-selective-photoetching experiments were performed with a 450 W xenon lamp (Ushio UXL 450SP). The wavelength of the light was tuned by using a series of cutoff filters: (1) 2.48 eV (Schott A490), (2) 2.73 eV (Schott A440), (3) 2.94 eV (Schott GG420), (4) 3.06 eV (Schott WG395), (5) 3.31 eV (Schott WG375), (6) 3.44 eV (Schott WG360), (7) 3.49 eV (Schott A350−1), (8) 3.54 eV (Schott A330), and (9) 4.08 eV (Schott A280). A cutoff filter absorbs photons of energies higher than the cutoff energy, while photons with a lower energy are transmitted. The cutoff energy is defined as the energy at which the transmission is 50% of the maximum transmission.

The suspensions were illuminated in a quartz container under continuous stirring and bubbling with oxygen. To avoid interference from extra absorption bands, methylviologen was not used in the experiments. The aqueous suspension of ZnS particles was illuminated without using a cutoff filter. The suspension of ZnO particles adsorbed on silica was first diluted 1:10 with water before it was illuminated while in a glass container, without using a cutoff filter. In this way the glass acts as a cutoff filter at about 4 eV.

Optical Characterization. Absorption measurements were performed on a Perkin-Elmer Lambda 16 UV/VIS spectrophotometer. The absorbance (A) was measured as the logarithm of the transmission ($T = I/I_0$) with water as a

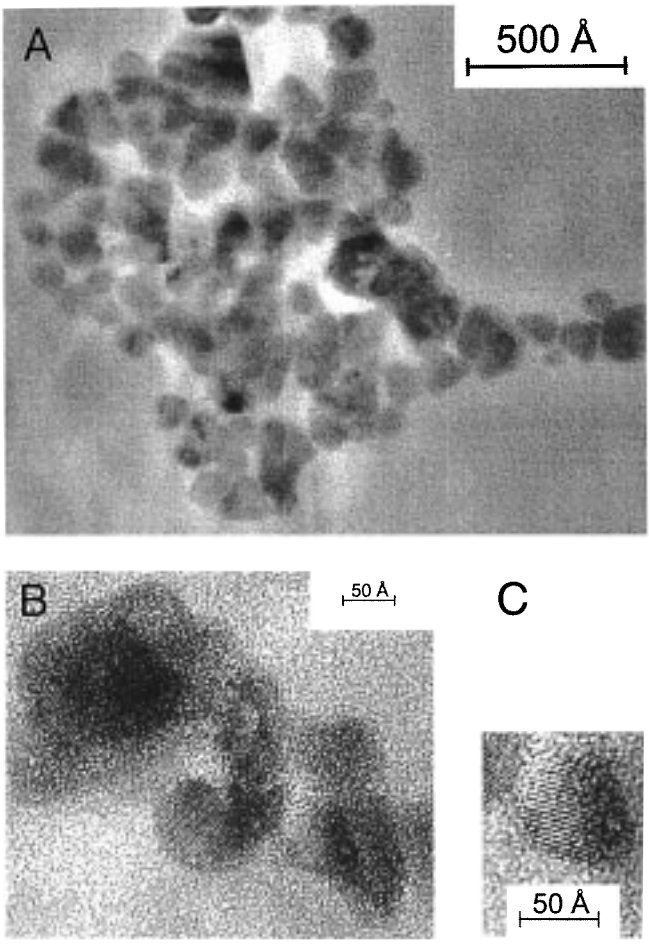

Figure 2. TEM micrographs of CdS particles from an aqueous suspension before illumination.

reference. Luminescence measurements were performed on a SPEX Fluorolog spectrophotometer model F2002 equipped with two double-grating 0.22 m SPEX 1680 monochromators and a 450 W xenon lamp as the excitation source.

Transmission Electron Microscopy. TEM measurements were performed on a Philips CM30 electron microscope operating at 300 kV. Only nonetched samples were used for these measurements. To perform TEM measurements on samples after photoetching, it is necessary to first remove the etch products (e.g. Cd^{2+} and SO_4^{2-} ions) from the suspension (e.g. by dialysis).

X-ray Powder Diffraction. XRD measurements were done using Cu $K\alpha_1$ radiation on a Philips PW1729 X-ray Generator equipped with a PW1710 Diffractometer Control.

IV. Results and Discussion

CdS. Figure 2 shows the results of TEM measurements on CdS particles. It is clear that the particles are crystalline, and lattice planes can be observed with interplanar distances of about 3.4 Å. These measurements also show that the particle size distribution is relatively broad. Due to cluster formation, it is difficult to determine a mean particle radius from the TEM measurements, but analysis shows many particles with radii between 30 and 40 Å.

XRD spectra show diffraction peaks that are broadened due to small crystal size. As a result of this broadening it is difficult to determine the crystal structure of the CdS particles: wurtzite or zinc blende. The interplanar distance of 3.4 Å occurs in both modifications. For bulk CdS, the most common modification

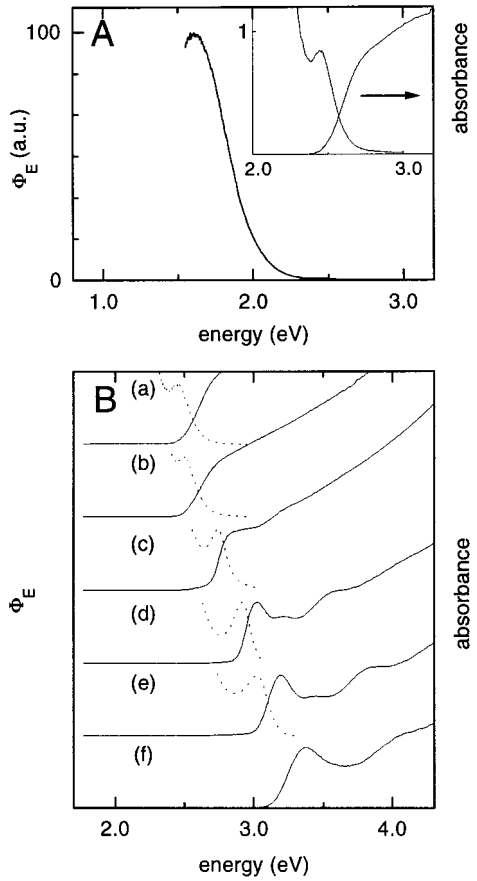

Figure 3. (A) Emission spectrum of an aqueous solution of nanocrystalline CdS particles upon excitation with 3.5 eV. The spectra were recorded before photoetching. The inset shows the exciton recombination band together with the absorption spectrum of the suspension. (B) Absorption (—) and emission (- - -) spectra of nanocrystalline CdS particles in aqueous suspension. Spectra a were recorded before illumination, spectra b—f after illumination for 2 h through filters with cutoff energies of 2.48, 2.73, 2.94, 3.06, and 3.31 eV, respectively. The intensities of the exciton recombination maxima and the first absorption maxima are set to unity. The emission spectra were recorded upon excitation with 4.1 eV radiation. Φ_E denotes the photon flux per constant energy interval.

is wurtzite.[39] For nanocrystalline CdS particles, both modifications have been reported, although the zinc blende structure is generally observed when CdS particles are prepared in solution.[27,38] For the strongest diffraction peak, using eq 3 with $\theta_B = 0.23$ rad and $B = 0.02$, a mean particle radius of 35 Å is obtained, which is in good agreement with the values obtained from TEM measurements and the value reported in the literature.[37]

For the wurtzite structure ($m_e^* = 0.22$, $m_h^* = 0.70$, and $\epsilon_\infty = 5.3$[39]), the Bohr radius of the exciton in bulk CdS calculated from eq 1 is 17 Å, while for the zinc blende structure ($m_e^* = 0.14$, $m_h^* = 0.51$, and $\epsilon_\infty = 5.3$[39]) a value of 26 Å is obtained. This means that the initial radius of our particles is close to that of the exciton in bulk CdS.

This is in agreement with the results obtained from absorption and luminescence measurements. Figure 3A

(39) Madelung, O. (Ed.) *Landolt-Börnstein, Numerical data and functional relationships in science and technology. Volume III-17: Semiconductors*; Springer-Verlag: Berlin, 1988; 17b pp 35—115, 166—194; 17f pp 155—161.

Table 1. Results of Size-Selective Photoetching of Nanocrystalline CdS Particles in Aqueous Suspension, Using Filters with Different Cutoff Energies

filter cutoff energy[a] (eV)	emission maximum (eV)	absorption onset[b] (eV)	absorption maximum (eV)	mean particle radius (Å)
[e]	2.45	2.47		35[c]
2.48	2.50	2.57		- - -
2.73	2.74	2.68	2.86	24
2.94	2.91	2.87	3.02	18
3.06	3.02	3.01	3.19	14
3.31		3.13	3.38	12
3.44		3.36	3.64	10
3.49		3.41	3.70	9.5
3.54		3.45	3.78	9.0
4.08	3.93		4.20[d]	7.5

[a] Defined at 50% of the maximum transmission. [b] Determined from extrapolating the steep part of the absorption spectrum. [c] Determined from TEM and XRD measurements. [d] Position of the lowest excitation maximum. [e] The first row contains the data for the CdS suspension before illumination.

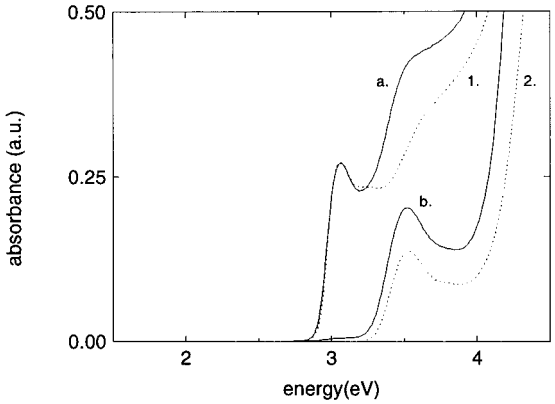

Figure 4. Absorption spectra of aqueous suspensions of nanocrystalline CdS particles after illumination through filters with cutoff energies 2.94 eV (1) and 3.31 eV (2), respectively. A 1:1 mixture of 1 and 2, shown as a, was again illuminated through a filter with cutoff energy 3.31 eV to yield b.

shows the absorption and emission characteristics of an aqueous suspension of nanocrystalline CdS particles before illumination. The onset of absorption, determined from extrapolation of the steep part of the spectrum, is at about 2.5 eV, similar to the value for the band gap energy of bulk CdS. The absorption spectrum is also structureless, indicating the presence of continuous energy bands. The emission spectrum shows an exciton recombination band centered at 2.45 eV, again indicating bulk behavior.

The spectra shown in parts a−f of Figure 3B refer to the same suspension, each after illumination for 2 h using filters with increasing cutoff energies. As the absorption spectra did not change upon prolonged illumination, the photoetching process was completed within this time span. Previously, it was reported that the use of methylviologen enhances the rate of the photoetching process.[31,32]

The spectra show a gradual shift of the absorption onset and a concomitant development of structure. These are clear indications of a decrease in size of quantum-confined semiconductor particles. The observation of structure is characteristic for a narrow size distribution.

Table 1 gives the values for the cutoff energies of the filters that were used, together with the energetic positions of the onset of absorption, first absorption maximum, and the position of the exciton recombination band in emission. The column on the right contains the particle size that was estimated from the empirical relationship between the first absorption maximum and mean particle radius.[10] The absorption and emission data from Table 1 show good agreement with the cutoff energies of the filters. This indicates that the particle size obtained after size-selective photoetching can be controlled by tuning the wavelength of the light.

From Table 1 and Figure 3B it is clear that upon photoetching the radius of the CdS particles gradually decreases below that of the bulk exciton. In comparison to the experiments described by Matsumoto et al.[30,31] and our previous work,[32] we have been able to adjust the particle size to much smaller dimensions by using light of higher energy. As can be seen in Table 1, nanocrystalline CdS particles could be photoetched to a radius as small as 7.5 Å, using light with an energy of 4.08 eV. These particles consist of approximately 50 CdS formula units, while the initial particles ($\langle R \rangle \sim 35$ Å) contain about 6500 CdS formula units.

To illustrate that size-selective photoetching can be used to narrow the size distribution of a suspension of nanocrystalline semiconductor particles, absorption measurements were performed on a mixture of two CdS suspensions. These suspensions were obtained by photoetching with light of 2.94 and 3.31 eV respectively. Figure 4 shows the absorption spectra of the separate suspensions (1 and 2) after a 1:1 dilution with water. Figure 4 also shows an absorption spectrum of a 1:1 mixture of undiluted 1 and 2 (spectrum a). The mixture was again illuminated through a filter with a cutoff energy of 3.31 eV, resulting in spectrum b. Because spectrum b resembles spectrum 2, it is clear that the particle size distribution narrows upon photoetching. Only the bigger particles added to suspension 2 from suspension 1 have been photoetched. The total area of the first absorption peak of spectrum b is a factor 1.85 that of the first absorption peak of spectrum 2. This means that the total number of particles has decreased slightly upon photoetching CdS particles from a radius of 18−12 Å. These results are not in agreement with those obtained by Matsumoto et al.[31] By analyzing the amount of sulfate ions produced during the photoetching process, they have concluded that the number of particles decreased to about 40% of the initial number of particles over the same size range as in our experiment.

At first sight one might think that a broadening of the first absorption band and the exciton recombination band indicates a broadening of the particle size distribution after photoetching. In Figure 5, it can be seen that the first absorption band broadens upon photoetching while the same effect is also visible in the emission spectra. Figure 6A contains two exciton recombination bands: after photoetching with 2.94 eV (a) and 4.08 eV (b). It is clear that the second emission band, originating from much smaller particles, is broader. The broadening of both absorption and exciton emission bands reflects the increasing dependence of the band gap energy on the particle size. This means that even particles with a relatively narrow size distribution can exhibit broad absorption and emission bands once they are in the strong confinement regime. The principle of

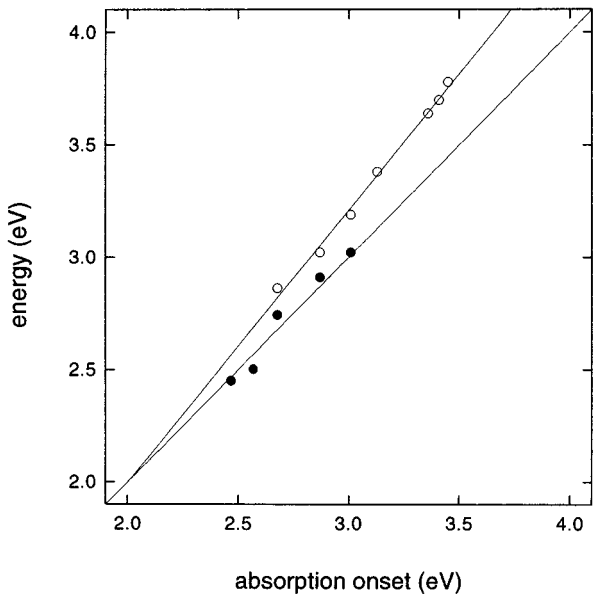

Figure 5. Energetic positions of the exciton recombination maximum (●) and the first absorption maximum (○) versus the absorption onset energy of nanocrystalline CdS particles in aqueous suspension.

broadening of the exciton emission band as a result of quantum confinement is illustrated in Figure 6B. The dependence of the lowest electronic transition in a semiconductor particle upon the particle size is shown in part a of Figure 6B. In part b of Figure 6B, three possible particle size distributions are shown (1−3) differing in mean particle size and/or monodispersity. The exciton emission bands, as shown in part c of Figure 6B, are constructed by plotting, for each particle size, the number of particles versus the energy for the lowest electronic transition (the intensity is taken as being proportional to the number of particles). In this way, only inhomogeneous line broadening is considered. It is clear that the widths of the emission bands originating from the smallest particles (b and c) are much larger than in the case of the bigger particles (a), even when the particle size distribution has narrowed.

A quantitative analysis of the change in particle size distribution can be performed by considering the width of the first absorption band. It is assumed that this band is inhomogeneously broadened due to a distribution in particle size. The experimental results obtained by Vossmeyer et al.[10] can be used to determine both the mean particle radius ($\langle R \rangle$) from the absorption maximum as well as the dispersion in particle size (ΔR) using the energy at which the absorption is half the maximum value on the low-energy side of the first absorption band. In Table 2 the values for $\langle R \rangle$ and ΔR are shown. It is clear that not only $\langle R \rangle$ but also ΔR decreases upon photoetching. As a result of size-selective photoetching, the dispersion in particle size decreased from 40% to 10−15%, which is comparable to that obtained by other techniques such as inverse micelle preparation and size-selective precipitation.[22,28,29]

Figure 5 also shows the increasing energy separation between the exciton recombination maximum in emission and the first absorption maximum, reflecting an increase in exciton binding energy with decreasing particle size. This size-dependence of the exciton binding energy has been reported before and was attributed to the enhanced spatial overlap between the electron and hole wave functions.[6]

As a result of this enhanced overlap, an increase of the oscillator strength with decreasing particle size is also expected[6] and has been observed.[10] Since the oscillator strength is linearly proportional to the absorption coefficient, absorption spectra can be used to study the size-dependence of the oscillator strength. In our case, all absorption spectra are recorded for the same suspension of nanocrystalline CdS particles, and only the particle size is changed by photoetching. In this way the change in oscillator strength due to a change in particle size can be determined accurately. In Figure 7, some of the absorption spectra from Figure 3B are replotted without scaling the absorption signal. It is clear that the total absorption signal decreases upon photoetching as a result of material being dissolved. The first absorption maximum can be fitted to a Gaussian curve, and the area of this curve, normalized for the particle volume, gives an indication for the absorption coefficient of the semiconductor particle per CdS unit. As the radius of the CdS particle decreases from 24 to 11 Å, the absorption coefficient (and therefore the oscillator strength) increases with a factor of 3.5. This is in good agreement with the experimental results obtained by Vossmeyer et al.[10] but not with the theoretical R^3-dependence.[6]

ZnS. Only XRD measurements were performed to characterize the ZnS particles. The diffraction pattern indicates that the ZnS particles have the zinc blende modification. This is in agreement with the fact that the wurtzite structure is the high-temperature modification of ZnS.[39]

From the strongest diffraction peak at $\theta_B = 0.25$ rad ($B = 0.03$ rad), a mean radius of 25 Å is determined for the ZnS particles. For bulk ZnS (zinc blende), using $m_e^* = 0.34$, $m_h^* = 0.5$ (both in units m_e), and $\epsilon_\infty = 5.4$,[39] eq 1 gives a Bohr radius of the exciton of about 15 Å.

Figure 8A contains the emission and absorption spectrum of an aqueous suspension of nanocrystalline ZnS particles before illlumination. There is no evidence for the presence of quantum size effects, as no structure is visible. Extrapolation of the steep part of the absorption spectrum yields an onset of 3.87 eV, while for bulk ZnS (zinc blende) the value for the band gap is 3.70 eV.[39] This discrepancy is most likely due to the error in the determination of the band gap energy from the absorption spectrum.

The emission spectrum shown in Figure 8A contains a broad trap emission band centered at 2.90 eV and no detectable exciton recombination band at the onset of absorption. An exciton recombination band appeared as a weak shoulder on the high- energy side of the broad emission band only after the surface of the ZnS particles was passivated with a ZnOH layer. Generally, these surface-passivated semiconductor particles cannot be photoetched.[32] This means that, in the case of (non-surface-passivated) ZnS, only absorption measurements can be used to study photoetching processes. As ZnS is a wide band gap semiconductor, photoetching experiments have to be carried out with light of a relatively high energy. A similar photoetching series as for CdS could not be made because few filters with high cutoff

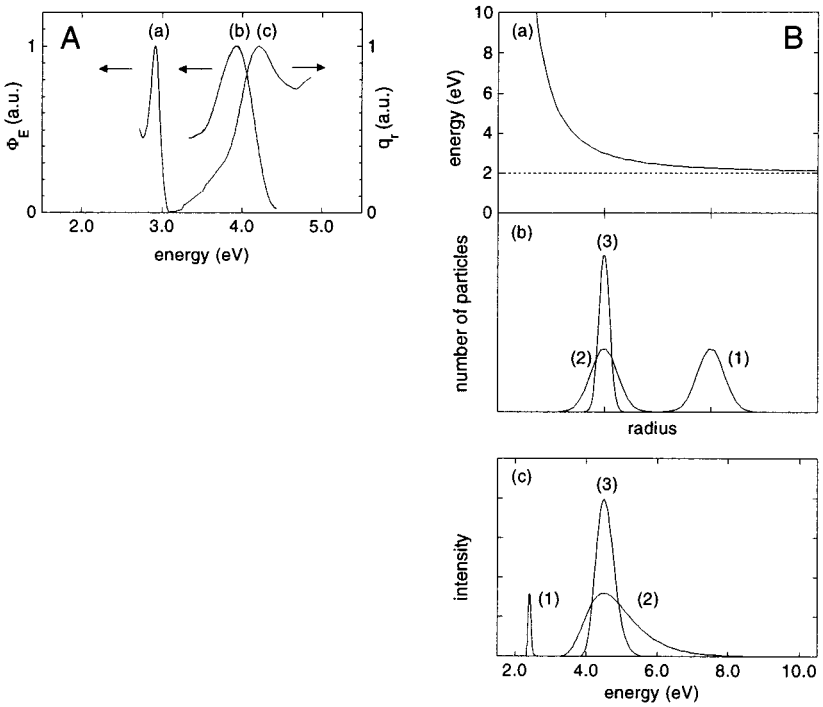

Figure 6. (A) Emission measurements on aqueous suspensions of nanocrystalline CdS particles showing the exciton recombination band. Spectrum a was taken after photoetching at 2.94 eV (exc 4.1 eV) and spectrum b after photoetching at 4.08 eV (exc 5.2 eV). Φ_E denotes the photon flux at constant energy interval. An excitation spectrum of the suspension that was photoetched at 4.08 eV (em 2.95 eV) is shown in c; q_r denotes the relative quantum output. (B) Illustration of the broadening of excitonic absorption and/or emission bands as a consequence of semiconductor particles becoming more quantum confined. The variation of the band gap energy with particle radius ($\sim R^{-2}$) is shown in a while b contains three possible particle size distributions, differing in mean particle size and monodispersity. The corresponding shapes of the excitonic absorption/emission bands are shown in c. The intensity is taken to be proportional to the number of particles. The homogeneous line broadening is considered to be negligible in comparison to the inhomogeneous line broadening.

Table 2. Mean Particle Radii ($\langle R \rangle$) and Accompanying ΔR^a Determined from the Energetic Positions of the Absorption Maxima and the Half-Maxima[10]

	absorption			
filter cutoff energy (eV)	maximum (eV)	half-maximum (eV)	$\langle R \rangle$ (Å)	ΔR (Å)
2.73	2.86	2.75	24	9
2.94	3.02	2.93	18	3
3.06	3.19	3.10	14	1.5
3.31	3.38	3.23	12	1.5
4.08	4.20[b]	3.92[b]	7.5	1

[a] Defined as half the fwhm of a Gaussian particle size distribution. [b] Determined from the lowest excitation maximum.

energies were available. From Figure 8B it is clear that, by using the xenon lamp without a cutoff filter, nanocrystalline ZnS particles can be photoetched. Upon illumination for 30 min the onset of absorption has shifted to 4.04 eV, and a structure has started to develop. At about 4.5 eV, a maximum of the first absorption band is visible. These results clearly indicate that upon photoetching the ZnS particles have entered the quantum confinement regime.

PbS. An interesting system for size-selective photoetching experiments is PbS. The band gap energy for bulk PbS is relatively low (0.41 eV), which means that photoetching experiments could be performed over a wide energy range, covering the IR to the UV spectral region. After preparation, absorption and luminescence measurements were performed to characterize the PbS suspensions. In Figure 9, curve a is the absorption spectrum of an aqueous suspension of nanocrystalline PbS particles. The absorption band at about 6 eV is

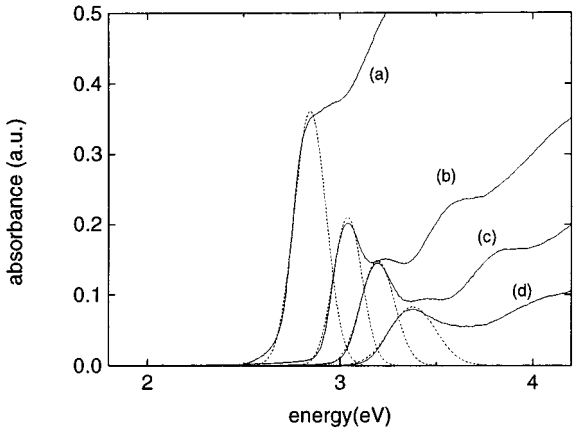

Figure 7. Absorption spectra of an aqueous suspension of CdS particles after photoetching at 2.73 eV (a), 2.94 eV (b), 3.06 eV (c), and 3.31 eV (d). The dashed curves are Gaussian fits to the first absorption maxima.

due to the presence of excess Pb^{2+} ions in solution. As the absorption starts at energies well above that of the bulk band gap and the spectrum shows structure, the PbS particles are clearly quantum confined. Because of the low effective masses of the charge carriers in PbS (m_e*, m_h* = 0.09[39]), eq 2 yields a value for the Bohr radius of the exciton in the bulk material of more than 200 Å. The three absorption maxima at 2.1, 3.3, and 4.3 eV probably result from different discrete energy levels.[11] Similar to ZnS, emission measurements on nanocrystalline PbS particles yielded only a broad trap emission band.

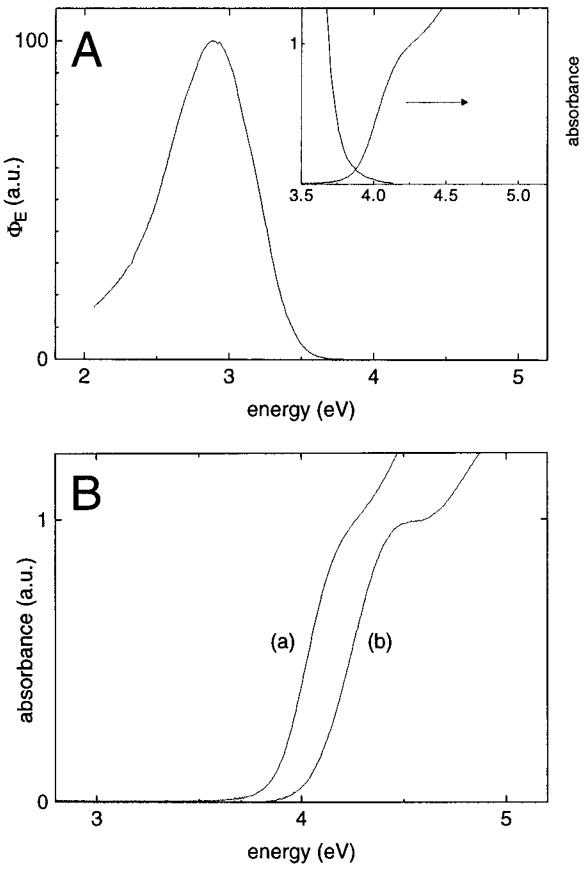

Figure 8. (A) Emission spectrum of an aqueous solution of nanocrystalline ZnS particles upon excitation with 5 eV. Φ_E denotes the photon flux at constant energy interval. The inset shows a part of the emission spectrum together with the absorption spectrum of the suspension. (B) Absorption spectra of an aqueous suspension of nanocrystalline ZnS particles before illumination (a) and after illumination for 30 min (b). Absorption spectrum b was scaled with respect to spectrum a.

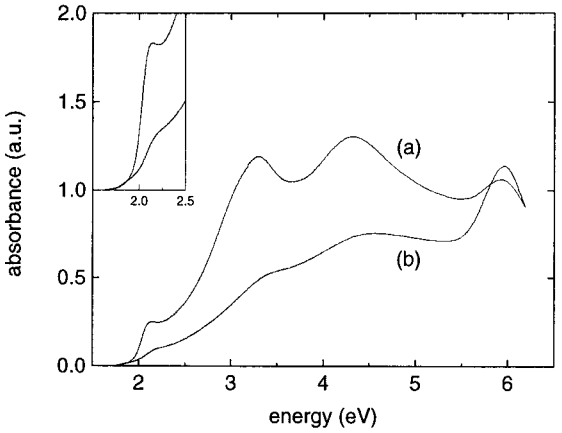

Figure 9. Absorption spectrum of an aqueous suspension of nanocrystalline PbS particles before illumination (a) and after illumination for 15 min using a filter with a cutoff energy of 2.25 eV (b). The inset is an enlargement of the onset of absorption.

From Figure 9 (curve b) it is clear that, upon illumination through a filter with a cutoff energy of 2.25 eV, the total intensity of the absorption signal decreases while at the same time the structure becomes much less pronounced. Although no distinct shift in the absorption onset is visible, it seems that the positions of the three maxima have shifted slightly toward higher energies. The loss of structure could be due to a broadening of the absorption bands. A possible reason for this broadening has already been addressed before for CdS. However, when illumination is continued for longer periods or with higher energies, the total absorption intensity goes down even further.

Two explanations could account for the above-mentioned observations. First, nanocrystalline PbS particles could be very difficult to photoetch due to the insolubility of $PbSO_4$ in water. Illumination of nanocrystalline PbS particles would then probably lead to the formation of a passivating sulfate layer that surrounds these particles and consequently inhibits further etching. However, this does not account for the observed decrease in absorbance upon prolonged illumination. A second explanation is based on the shape of the PbS particles. According to the literature,[11] the particles have a rodlike shape. The length of these rods is about 180 Å, which is fairly close to the value for the Bohr radius of the exciton in bulk PbS (~200 Å). When illumination of the PbS particles leads to a shortening instead of a narrowing of the rods, photoetching might not influence the positions of the absorption bands, but the total absorption signal will decrease as the PbS particles are dissolving. However, from TEM measurements that we performed it was clear that the PbS particles did not have a rodlike shape but were almost spherical.

In contrast to the experimental results on CdS and ZnS, the results on nanocrystalline PbS particles do not provide concrete evidence for the possibility of size-selective photoetching for these particles.

ZnO. TEM measurements were performed to characterize the ZnO particles, and TEM images are shown in Figure 10. It is clear that the particles are crystalline with interplanar distances of about 3.3 Å. As in the case of CdS, these measurements only allow a rough estimation of the mean particle radius, which is about 30 Å. According to the literature, the Bohr radius of the exciton for bulk ZnO is equal to 19 Å.[39]

Figure 11A shows the emission spectrum of an aqueous suspension of ZnO particles adsorbed on silica. This spectrum contains two bands: a broad trap emission band centered at 2.08 eV and an exciton recombination band centered at 3.42 eV. The position of the exciton recombination band corresponds to the value reported in the literature for the band gap of bulk ZnO (values between 3.2 and 3.4 eV[2,13,39]). Figure 11A also shows the absorption spectrum of the suspension. Extrapolation of the steep part of the absorption spectrum gives an onset of 3.38 eV. Using an experimental relationship between the onset of absorption and the particle radius,[14] an onset of 3.38 eV corresponds to a particle radius of 35 Å, which is in good agreement with our TEM measurements but larger than reported in the literature for a similar preparation.[13] For ZnO particles in this size range, the energetic position of the onset of absorption varies only very slightly with particle size. Therefore, the error in the calculated value for the mean radius of the ZnO particles is relatively large.

Photoetching experiments were performed using glass as a cutoff filter at 4 eV. These experiments show that nanocrystalline ZnO particles can be photoetched while

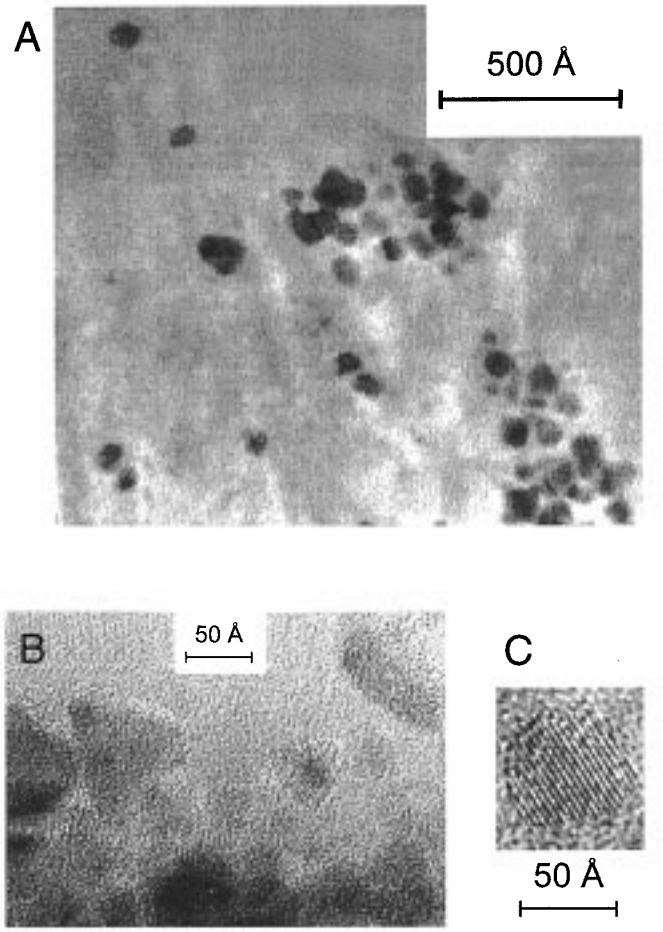

Figure 10. TEM micrographs of ZnO particles from a suspension in 2-propanol.

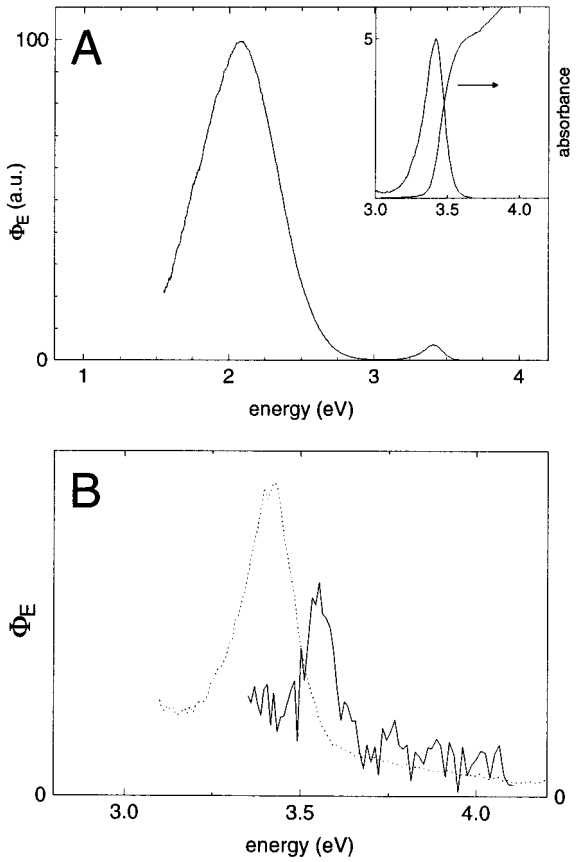

Figure 11. (A) Emission spectrum of an aqueous solution of nanocrystalline ZnO particles. The inset shows the exciton recombination band together with the absorption spectrum of the suspension. (B) Emission spectra showing the exciton recombination bands of an aqueous suspension of ZnO particles before illumination (dashed line) and after illumination (solid line) for 16 h through glass with a cutoff energy of about 4 eV. The emission spectrum after illumination was multiplied by a factor 10. Φ_E denotes the photon flux per constant energy interval. The emission spectra were recorded upon excitation with 4.1 eV.

in aqueous suspension. Figure 11B shows the shift of the exciton recombination band from 3.42 to 3.55 eV upon illumination for 16 h. This shift indicates that the ZnO particles have become smaller and have entered the quantum confinement regime. After photoetching, the ZnO particles were very unstable, as the exciton recombination band disappeared with time. It was not possible to record an absorption spectrum of the ZnO suspension after illumination because the signal had become too low due to the loss of material during the photoetching process.

Similar to CdS, more information about the mean particle size and the particle size distribution can be obtained by using an empirical relationship between the onset of absorption and the particle size for ZnO particles.[14] In our case, emission measurements have to be used instead of absorption measurements. To be able to use the relationship it is assumed that the shift between the maximum of the exciton recombination band and the onset of absorption is the same before and after photoetching. In this way, we have determined that a mean particle radius of 35 ± 15 Å before photoetching is decreased to 15 ± 5 Å after photoetching. It is clear that not only the mean particle size has decreased upon photoetching but also the particle size distribution has been narrowed.

As can be seen in Figure 11B, the width of the exciton recombination band has become slightly smaller upon photoetching. At a radius of 15 Å, the ZnO particles have not yet entered the range in which the band gap energy depends very strongly on the particle size. According to Haase et al.,[14] a strong dependence of the absorption onset on particle size starts at a particle radius of about 10 Å, corresponding to an absorption onset of about 3.6 eV.

V. Conclusion

The experiments described in this paper demonstrate the feasibility of size-selective photoetching as a means to adjust the size of nanocrystalline semiconductor particles with a high degree of control. The particle size after photoetching is determined by the energy of the light that is used for photoetching.

The technique works very well for nanocrystalline CdS particles and enables one to prepare a series of samples with different well-defined particle radii, covering a wide range from 35 to 7.5 Å. The decrease in mean particle size is accompanied by a narrowing of the particle size distribution from some 40% to 10−15%.

The applicability of the technique to nanocrystalline semiconductor particles of ZnS and ZnO has been demonstrated, but the wide band gap of these compounds limits the range for size-selective-photoetching experiments.

Nanocrystalline PbS particles are very difficult to photoetch, most probably due to the insolubility of $PbSO_4$ in water, which could result in the formation of a passivating sulfate layer surrounding the PbS particles.

Acknowledgment. The authors would like to thank Prof. Dr. A. Henglein for many useful suggestions concerning the experiments. Dr. M. A. Verheijen from the Philips Centre for Manufacturing Technology is acknowledged for performing the TEM measurements on CdS and ZnO particles. The investigations were supported by The Netherlands Foundation for Chemical Research (SON) with financial aid from The Netherlands Organization for Scientific Research (NWO).

CM980715P